Journal of Membrane Science 614 (2020) 118529

Contents lists available at ScienceDirect

Journal of Membrane Science

journal homepage: http://www.elsevier.com/locate/memsci

Preparation of carbon molecular sieve membranes with remarkable CO_2/CH_4 selectivity for high-pressure natural gas sweetening

Linfeng Lei [a], Arne Lindbråthen [a], Xiangping Zhang [b], Evangelos P. Favvas [c], Marius Sandru [d], Magne Hillestad [a], Xuezhong He [a,e,*]

[a] Department of Chemical Engineering, Norwegian University of Science and Technology, NO-7491, Trondheim, Norway
[b] Beijing Key Laboratory of Ionic Liquids Clean Process, Institute of Process Engineering, Chinese Academy of Sciences, P.O. Box 353, Beijing, 100190, China
[c] Institute of Nanoscience and Nanotechnology, National Center for Scientific Research "Demokritos", Aghia Paraskevi, 153 41, Athens, Greece
[d] SINTEF Industry, SINTEF AS, NO-7465, Trondheim, Norway
[e] Department of Chemical Engineering, Guangdong Technion Israel Institute of Technology (GTIIT), 241 Daxue Road, Shantou, 515063, China

ARTICLE INFO

Keywords:
Carbon hollow fiber membranes
Cellulose
Ionic liquids
Natural gas
CO_2 removal

ABSTRACT

Carbon hollow fiber membranes (CHFMs) were fabricated based on cellulose hollow fiber precursors spun from a cellulose/ionic liquid system. By a thermal treatment on the precursors using a preheating process before carbonization, the micropores of the prepared CHFMs were tightened and thus resulting in highly selective carbon molecular sieve (CMS) membranes. By increasing the drying temperature from RT to 140 °C, the cellulose hollow fiber precursors show a substantial shrinkage, which results in a reduction of average pore size of the derived CHFMs from 6 to 4.9 Å. Although the narrowed micropore size causes the decrease of gas diffusion coefficient, stronger resistance to the larger gas molecules, such as CH_4, eventually results in an ultra-high CO_2/CH_4 ideal selectivity of 917 tested at 2 bar for CHFM-140C due to the simultaneously enhanced diffusion and sorption selectivity. The CHFM-140C was further tested with a 10 mol%CO_2/90 mol%CH_4 mixed gas at 60 °C and feed pressure ranging from 10 to 50 bar. The obtained remarkable CO_2/CH_4 separation factor of 131 at 50 bar and good stability make these carbon membranes great potential candidates for CO_2 removal from high-pressure natural gas.

1. Introduction

Natural gas is considered one of the most attractive low carbon energy sources due to its availability, versatility and environmental benefit. However, raw natural gas produced from gas wells/reservoirs usually contains impurities such as carbon dioxide (CO_2), hydrogen sulfide (H_2S), water, and heavy hydrocarbons (HHCs), which need to be removed or reduced before being transported and distributed to natural gas grids as those impurities will cause a series of issues related to pressure drop, plugging of a pipeline, and pipeline corrosions [1]. Amine absorption is the state-of-the-art technology for CO_2 removal from natural gas, but it faces high capital and operating cost, complex operation process, and environmental pollution [2]. Membrane separation process is considered as a very promising technology for natural gas sweetening in remote regions where small footprint, flexibility, and less maintenance are highly desirable [3,4]. Various membrane materials have been developed for CO_2 removal from natural gas, including glassy polymer membranes [5,6], metal-organic framework (MOF)-based hybrid membranes [7–9], fixed-site-carrier (FSC) membranes [10,11] and carbon molecular sieve (CMS) membranes [3,4,12,13]. Some polymeric membranes such as cellulose acetate, polyimide, and perfluoro membranes have been successfully used for industrial natural gas sweetening [2,4]. However, in addition to being faced with permeability−selectivity trade-off [14], the loss of selectivity at high operating pressure due to CO_2 and HHCs plasticization as well as membrane compaction [15] is another challenge for polymeric membranes. For instance, CO_2/CH_4 selectivity of cellulose acetate membrane drops by 70% when exposed to a high pressure natural gas stream containing hydrocarbon contaminants [3]. The reduction of selectivity would lead to a lower separation efficiency, and thus requires a higher energy consumption to achieve the requirement of product purity. Moreover, low selectivity will also cause a high CH_4 loss, which may lead to a significant environmental impact due to a greater greenhouse effect of CH_4 compared to CO_2. Thus, it is important to develop highly CO_2 selective membranes to address the

* Corresponding author. Department of Chemical Engineering, Norwegian University of Science and Technology, NO-7491, Trondheim, Norway.
E-mail addresses: xuezhong.he@ntnu.no, xuezhong.he@gtiit.edu.cn (X. He).

https://doi.org/10.1016/j.memsci.2020.118529
Received 17 May 2020; Received in revised form 28 June 2020; Accepted 23 July 2020
Available online 29 July 2020

challenges on membranes for high-pressure (usually >50 bar) natural gas sweetening.

Among different membrane materials, CMS membranes with rigid pore structures, fabricated by controlled carbonization of polymeric precursors at high temperature, have shown attractive separation performances for CO_2 removal from natural gas [3]. The bimodal pore structure of ultramicropores and micropores in CMS membranes provides a high CO_2/CH_4 separation performance with both high CO_2/CH_4 selectivity and CO_2 permeability [16,17]. Besides, the microstructures in the CMS membranes can be adjusted to enhance the selectivity further. Qiu et al. [18] reported an expedited physical aging process, named to "hyperaged", to reduce the micropores of CMS membranes. When freshly prepared carbon hollow fiber membranes (CHFMs) were hyperaged by hot air flow at the temperature range between 90 °C and 250 °C, it was found that the distance of adjacent carbon strands was compressed, and thereby resulting in smaller ultramicropores. As a result, a selectivity of H_2/C_2H_4 was increased more than a 10-fold compared with the freshly prepared CHFMs. Tightening micropores of CMS membranes by elevating carbonization temperature has been widely used to obtain more selective membranes [16,17,19–22]. For example, by increasing the carbonization temperature from 750 to 900 °C, the selectivity of CO_2/CH_4 for a polyimide derived CMS membrane was improved from 15 times as reported by Zhang and Koros [16]. The improved selectivity was attributed to synergistically enhanced sorption selectivity and diffusion selectivity. However, higher carbonization temperatures normally lead to more brittle and inflexible CMS membranes [23], which can cause extra difficulty on the membrane handling and membrane module assembly [24]. In addition to optimizing carbonization conditions (e.g. carbonization temperature, carbonization atmosphere, heat rate and soak time), modification of the precursors has also been studied to improve selectivity [25–28]. Among them, Park et al. [26] found that the microstructure of the polyimide precursors could significantly determine the separation performance of the derived CMS membranes. By reducing the fractional free volume (FFV) of polyimides, the pore size of the precursors was reduced, which resulted in a more selective carbon membrane [26]. Moreover, by blending two thermally stable polymers of polyetherimide (PEI) and polyimide to tune microstructure of precursor, both gas separation selectivity and permeability of prepared CMS membranes were improved [27]. However, most of the reported methods for tuning precursors are based on chemical modification, which may increase the fabrication complexity and increase the production cost for CMS membranes. Recently, cellulose precursors have been studied for the fabrication of CMS membranes, and shows high selectivity for gas separations [4,29]. Instead of drying wetted-cellulose hollow fiber from water directly, the precursors were immersed in a glycerol aqueous solution before drying, which is used to prevent the curling and pore collapse of cellulose hollow fibers [4]. However, glycerol can act as a membrane pore radius-maintaining agent by filling the micropores [30,31]. The carbon membranes prepared from glycerol-containing cellulose precursors may form relatively large micropores. Thus, in order to obtain a denser structure of precursor for the fabrication of highly selective CMS membranes, proper protocols for glycerol removal should be identified.

In this work, a drying pretreatment method was used to remove glycerol and water inside cellulose precursors to enhance the crystallinity of cellulose precursor and then making CMS membranes with narrower pore size to improve gas selectivity. The CO_2/CH_4 selectivity increases 4.7 times for the CHFMs fabricated from the precursors with a higher drying temperature of 140 °C compared to that made from the cellulose precursors dried at 80 °C. A remarkable CO_2/CH_4 separation factor of 131 obtained from the mixed gas (10% CO_2/90% CH_4) permeation measurement at 60 °C and 50 bar shows attractive a great potential for high-pressure natural gas sweetening.

2. Experimental

2.1. Materials

Microcrystalline cellulose (MCC, Avicel PH-101), dimethylsulfoxide (DMSO) (≥99%) and glycerol (>99%) were purchased from Sigma-Aldrich. The Institute of Process Engineering, Chinese Academy of Sciences (IPE-CAS) provided 1-Ethyl-3-methylimidazolium Acetate (EmimAc) for direct use without further treatment, and the product purity was confirmed by ^1H and ^{13}C NMR [32]. MCC and EmimAc were dried in a vacuum oven at 80 °C for 48 h to eliminate residual moisture. Tap water was used as a coagulation solvent during spinning. Single gas (e.g., CO_2 and CH_4) and 10 mol%-90 mol.% CO_2/CH_4 mixed gas were purchased from AGA, Norway.

2.2. Fabrication of carbon hollow fiber membranes

A dope solution with 12 wt% MCC/88 wt% (EmimAc + DMSO) was used to fabricate cellulose hollow fibers by a dry-wet spinning technique under the conditions listed in Table 1. Binary mixtures of ionic liquids-molecular solvents can enhance solubility as reported by Tomimatsu et al. [33]. By diluting the ionic liquids with DMSO, MCC solubility will be increased due to the corresponding increase of ion mobility [34]. However, it should be noted that the cellulose dissolving ability decreases dramatically when IL content is lower than 20 mol.% of the mixed solvent, probably due to the trade-off of the solvation of the $[Emim]^+$ cation by DMSO and the cellulose dissolution by the $[Ac]^-$ anion of IL [33]. On the other hand, too high EmimAc concentration will cause the reduction of cellulose solubility and also increase the viscosity of dope solution as the low mobility of ions can restrict the penetration of ILs between cellulose chains [35]. Therefore, the binary solvent system with a moderate IL content (i.e., the weight ratio of DMSO and EmimAc was 3:1) was prepared for MCC dissolution in this work. The detailed procedure of dissolving MCC in EmimAc/DMSO was described elsewhere [4]. The spun cellulose hollow fibers were then rinsed in water baths for 72 h (during that time the water was replaced three times with fresh water) to remove residual solvents, and subsequently conducting solvent exchange by soaking hollow fibers in a 10 wt% glycerol aqueous solution for 48 h. The obtained cellulose hollow fibers were dried at room temperature (RT, 20–25 °C) for 12 h and subsequently used as precursors (Cellulose-RT) for carbon membranes. Another two batches of precursor fibers were obtained by drying the cellulose hollow fibers in a convection oven at 80 °C and 140 °C, respectively. These precursors are named correspondingly Cellulose-80C and Cellulose-140C. Afterward, CHFMs were prepared by carbonization of the dried cellulose hollow fiber precursors via a controlled procedure in a tubular furnace (Horizontal Split Tube Furnace, Carbolite Gero Limited) with a continuous flow of 80 mL min^{-1} CO_2 purge gas as shown in Fig. 1. The tubular furnace was firstly evacuated and then purged with CO_2 to remove other gases before carbonization. The carbonization condition was based on the previous work on the carbonization of cellulosic-based precursors. It was reported that both purge gas and the final temperature has a more significant effect on the carbon membrane structure and performance compared to the heating rate and final soak

Table 1
Spinning conditions for the fabrication of cellulose hollow fibers.

Spinning condition	Value
Air gap (mm)	50
Dope solution flow (ml min^{-1})	4.4
Bore composition (water concentration, wt.%)	20
Bore fluid flow (ml min^{-1})	2.4
Take-up speed (m min^{-1})	7.3
Dope temperature (°C)	50
Coagulation temperature (°C)	25
Spinneret size, OD/ID (mm)	0.7/0.5

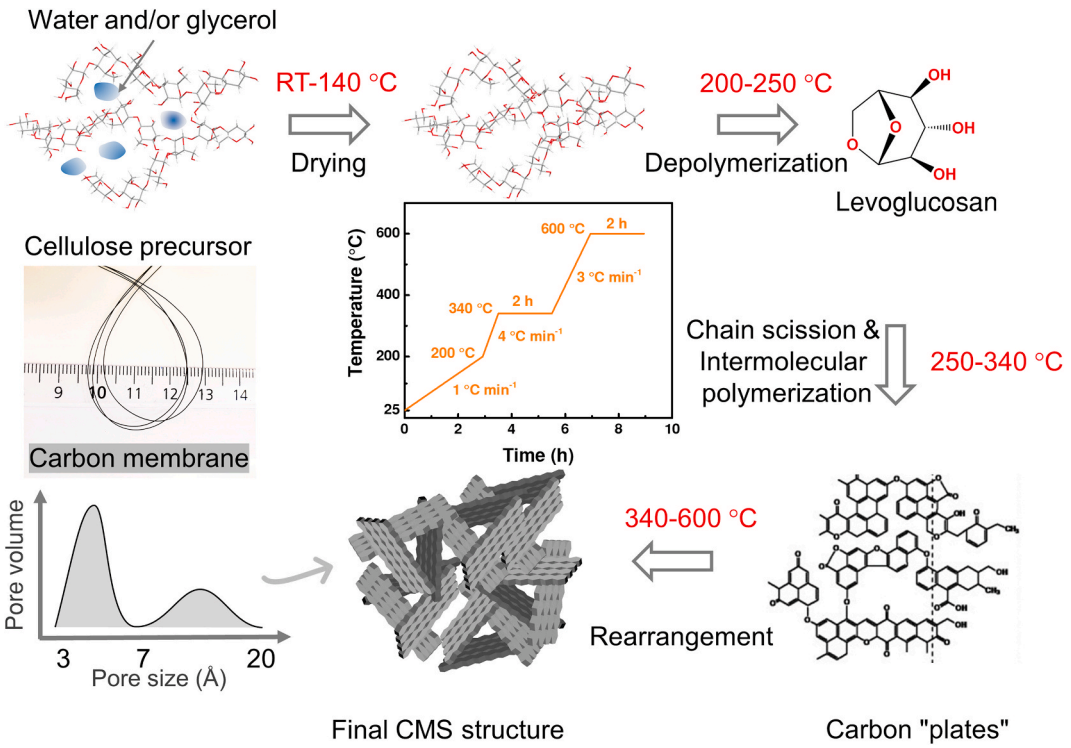

Fig. 1. The proposed transforming mechanism from cellulose precursors to CMS membranes. The insert picture shows the flexibility of CHFMs with a ca. 1 cm bended radius.

time [22,36]. Applying CO_2 purge gas will lead to carbon membranes with higher micropore volume to provide enhanced gas permeability compared to inert gases like N_2 for cellulosic precursors. Moreover, higher carbonization temperature can potentially enhance the membrane selectivity due to sintering and condensation effect, while a lower final temperature may lead to the carbon membranes with higher gas permeability. Thus, considering the balance of both CO_2 permeability and CO_2/CH_4 selectivity, the moderate final temperature of 600 °C was applied in this work. During the carbonization process, the physical desorption and dehydration occur at a temperature below 200 °C to remove both free and bound water. After that, the cleavage of the 1, 6-glycosidic linkages occurs at ca. 200–250 °C, where cellulose is depolymerized to form levoglucosan. Following the continuous increase of temperature using a heating rate of 4 °C min^{-1}, carbon "plates" with less-ordered microstructure will be formed due to the chain scission and intermolecular polymerization of cellulose at 250–340 °C, and further leads to the formation of micropores during the 2 h soaking at 340 °C. Those micropores can be further rearranged and aged through internal condensation at higher carbonization temperatures of 340–600 °C at a heating rate of 3 °C min^{-1}. After 2 h soaking at the final temperature of 600 °C, turbostratic carbon membranes containing both micropores and ultramicropores will be formed as illustrated in Fig. 1. The CHFMs are flexible with a bended radius of ca. 1 cm, as shown in Fig. 1, which shows great potential in the membrane module upscaling.

2.3. Characterization

The cross-sectional images of CHFMs were obtained by a scanning electron microscopy (SEM, Hitachi TM3030 tabletop microscope). Thermogravimetric analysis (TGA, TG 209F1 Libra) was employed to investigate the weight loss of different cellulose precursors as a function of pyrolysis temperature. Samples were heated from 30 to 600 °C at a heating rate of 5 °C min^{-1} under N_2. X-ray diffraction (XRD, Bruker D8 Focus) analysis of cellulose hollow fiber precursors was conducted at 45 kV and 200 mA with 2θ ranging from 5° to 70° at a scan speed of 0.05 s^{-1} (Cu-Kα radiation, λ = 0.154 nm). The crystallinity index (*CrI*) of cellulose hollow fiber precursors were estimated by the following Eq. (1) [37,38],

$$CrI = \frac{I_{total} - I_{am}}{I_{total}} \times 100\% \quad (1)$$

where I_{total} the scattered intensity at the main peak, located at around 2θ = 20.1°, and I_{am} is the scattered intensity related to the amorphous region, located at around 2θ = 14.5°.

Gas sorption isotherms of pure CO_2 and CH_4 for CHFMs were obtained at 25 °C up to 15 bar using a TA Rubotherm magnetic suspension balance (MSB). The average pore size and micropore volume of the prepared CHFMs were estimated by Dubinin-Radushkevitch (DR) equation (Eq. (2)) [39] and the Stoeckli equation (Eq. (3)) [40],

$$\frac{w}{w_0} = \exp\left(-\left(\frac{RTln\left(\frac{p_0}{p}\right)}{\beta E_0}\right)^2\right) \quad (2)$$

$$L_0 = \frac{10.8\ (nm \cdot kJ/mol)}{E_0 - 11.4\ (kJ/mol)} \quad (3)$$

In which w ($cm^3\ g^{-1}$) and w_0 ($cm^3\ g^{-1}$) are the volume of adsorbed CO_2 and micropore volume of CHFMs, respectively. Fugacity was used instead of pressure at high pressure. E_0 (kJ mol^{-1}) and L_0 (Å) are corresponding to the adsorption activation energy and average micropore size, respectively. The affinity coefficient (β) used in the DR equation is 0.35 according to the literature [39,41]. To determine the sample true density (ρ_s), buoyancy measurements with non-absorbable helium were conducted by MSB. Subsequently, bulk density (ρ_b) is calculated by Eq. (4),

$$\frac{1}{\rho_b} = \frac{1}{\rho_s} + \omega_0 \quad (4)$$

Gas sorption coefficients (cm^3 (STP) cm^{-3} $cmHg^{-1}$)) of CHFMs at 2 bar were derived from the gravimetric sorption isotherms.

2.4. Gas permeation measurements

Single gas permeation testing for CHFMs was conducted at 25 °C under a 2 bar upstream pressure using the constant downstream volume method [4]. Membrane modules were degassed under vacuum for about 6 h to release potential adsorbed molecules from all adsorption sites. For each type of CHFM, three membrane modules were tested to obtain the average gas permeabilities. Gas permeability is calculated using Eq. (5):

$$P = \frac{273 \times 10^7 V \cdot r_1 ln\left(1 + \frac{l}{r_1}\right)}{76T \cdot A_{inner} \cdot P} \cdot \frac{dp}{dt}^{steady} \quad (5)$$

where P (Barrer, 1 Barrer $= 1 \times 10^{-10}$ cm^3(STP) $\cdot cm \cdot cm^{-2} \cdot s^{-1} \cdot cmHg^{-1} = 3.382 \times 10^{-16}$ $mol \cdot m \cdot s^{-1} \cdot m^{-2}$ Pa^{-1}) is the single gas permeability. V (cm^3) is the permeate volume, and T (K) is the membrane testing temperature. A_{inner} (cm^2) is the inner active surface area of CHFMs (bore-side feeding). r_1 (cm) and l (cm) are the inner radius and the thickness of carbon membranes. $\triangle P$ is the trans-membrane pressure difference between upstream and downstream. $\frac{dp}{dt}_{steady}$ is corresponding to the pressure increasing rate at steady-state by subtracting system leakage. The CO_2/CH_4 ideal selectivity (permselectivity) is calculated by the permeability ratio of CO_2 to CH_4.

A 10 mol%-90 mol% CO_2/CH_4 mixed gas was used to investigate the separation performances of CHFMs at 60 °C with a total pressure ranging from 10 to 50 bar. The membrane modules were operated in a counter-current flow pattern (i.e., feed gas flowing in one direction and permeate gas is collected in the opposite direction using N_2 as sweep gas) by using a high-pressure permeation rig described elsewhere [4]. In brief, the gas mixture at 200 mL min^{-1} was fed from the bore side of the modules with the membrane areas of 10 cm^2. It should be noted that bore-side feeding may provide better gas distribution and enhanced gas transfer coefficient [42] as a higher gas velocity in the bore side can be achieved for the lab-scale modules with low packing density compared to the shell-side feeding. Moreover, bore-side feeding is performed in parallel to the longitudinal axis of the fiber which greatly reduces the module inlet shear stresses (and potential vibration resonance) on the individual fibers that the perpendicular shell-side feeding may induce. The permeate gas composition and flow rate exited from the shell side together with a 30 mL min^{-1} sweep gas at 1 bar were analyzed by a gas chromatograph (GC, 8610C) and a bubble flow meter, respectively. Each experiment was recorded after the permeate composition stabilized. The separation factor was calculated by $\alpha_{CO_2/CH_4} = \frac{y_{CO_2}/y_{CH_4}}{x_{CO_2}/x_{CH_4}}$, in which y_i and x_i are the concentrations of the components in the permeate and feed, respectively.

3. Results and discussion

3.1. Membrane morphology

The cross-sectional SEM images of different cellulose hollow fiber precursors (i.e., Cellulose-RT, Cellulose-80C, and Cellulose-140C) and the derived CHFMs (CHFM-RT, CHFM-80C and CHFM-140C) are depicted in Fig. 2, which show macrovoids-free and symmetric structures. It can be seen that the cellulose precursors present symmetric structures without the difference in the inner and outer sides as indicated in Fig. S1, which results in the corresponding symmetric carbon membranes after carbonization. The dimension of the precursors presents a decrease of the outer diameter from 460 μm for Cellulose-RT to 384 μm for Cellulose-140C, as shown in Fig. 2a–c and Table 2. Moreover, the shrinkage of wall thickness from 96 to 84 μm also indicates that the precursor of Cellulose-140 has a denser structure compared to the Cellulose-RT. Furthermore, the diminution of the outer diameter dimensions of the derivatives carbon membranes was recorded equal to 45.7, 39.5 and 36.4% for the Cellulose-RT to CHFM-RT, Cellulose-80C to CHFM-80C and for the Cellulose-140C to CHFM-140C respectively. The smaller values in diameter dimension were caused by the higher drying temperatures which were applied at the precursors to remove glycerol and water inside cellulose. Recently, Falca et al. [43] reported that an interconnected micropore structure observed by a Cryo-SEM exists in wet water-filled cellulose membranes. However, the micropores collapsed during the drying process and afterward, showed a dense structure in the dried state. Besides, the abundant hydrogen bonds in membranes such as cellulose-cellulose groups, water-cellulose groups, water -water molecules, play an important role in the morphology change during the water desorption. In this work, the glycerol acts as a membrane pore radius-maintaining agent by filling the micropores to prevent collapsing [31]. On the other hand, when elevating drying temperature, the water maintained in cellulose by glycerol was gradually removed, thereby the inter-cellulose hydrogen bonds (which were broken upon water adsorption) will reform [44] and thus potentially resulting in a denser cellulose chain packing. Following the same carbonization protocol, three types of CHFMs were obtained as shown in

Table 2
The characteristics of cellulose hollow fiber precursors.

Precursor	Weight loss (%)	Crystallinity index (%)	Average outer diameter (μm)	Average thickness (μm)
Cellulose-RT	86.4	60.2	460	96
Cellulose-80C	79.5	62.0	417	89
Cellulose-140C	77.0	64.1	384	84

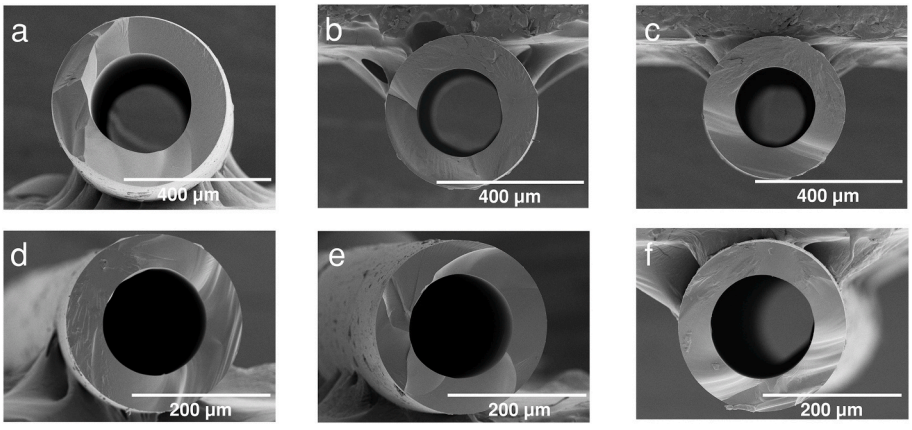

Fig. 2. Cross-sectional SEM images of cellulose hollow fiber precursors and CHFMs. a-c) cellulose hollow fiber precursors dried at RT, 80 °C, and 140 °C, corresponding to Cellulose-RT, Cellulose-80C and Cellulose-140C. d-f) CHFMs derived from a), b) and c) corresponding to CHFM-RT, CHFM-80C and CHFM-140C.

Fig. 2d–f of the cross-sectional images with similar dimensions (outer diameter of ~245 μm, the thickness of ~45 μm).

3.2. Properties of cellulose hollow fiber precursor

The thermal stability of cellulose hollow fiber precursors dried at different temperatures was investigated by TGA, as shown in Fig. 3a. The drying and thermal degradation can be divided into four regions: (i) release of free water presented inside membrane at below 120 °C; (ii) release of bound water and glycerol at 120–200 °C; (iii) cellulose degradation occurs at ~ 200 °C and starts to form pore network; (iv) degradation rate starts to decline when decomposition temperature is above 340 °C. Compared to the cellulose hollow fibers dried at RT, the precursors dried at the higher temperatures of 80 °C and 140 °C have relatively lower solvent (water + glycerol) contents and thus resulting in a less weight loss as shown Table 2 (The TGA curves of Cellulose-100C and Cellulose-120C (dried at 100 and 120 °C, respectively), shown in Fig. S2, indicate that the solvents of glycerol and water are gradually reduced). When water-filled cellulose hollow fiber precursors have immersed in glycerol aqueous solution, the membrane surface was covered by glycerol. Thus, after drying at room temperature, the free water in membranes evaporates slowly, while glycerol whereas is still kept inside the free volume of the cellulose matrix [30]. When the cellulose hollow fibers are dried at the higher temperature (i.e., Cellulose-80C and Cellulose-140C), both glycerol and bound water starts to release, which leads to the shrinkage of precursors. Furthermore, during the release of bound water, the cellulose interchain hydrogen bonds start to reform concomitantly to accelerate pore shrinkage as well. Since most of the water and glycerol have been removed from the precursor of Cellulose-140C, it presents a denser structure compared to the other two precursors of Cellulose-RT and Cellulose-80C. The characteristic peaks, measured by XRD, located at $2\theta = 12.1°$, 20.1° and 21.8°, corresponding to the ($\bar{1}$ 0 0), (1 1 0) and (0 2 0) planes as shown in Fig. 3b, indicates that the prepared cellulose hollow fiber precursors are cellulose II [45,46]. Moreover, with the increase of drying temperature, the characteristic peaks of ($\bar{1}$ 0 0) and (0 2 0) plane of the precursors become stronger. The *CrI* of different precursors are increased from 60.2 to 64.1% calculated by Eq. (1), which indicates that the crystallinity of the precursors dried at higher temperatures (e.g., Cellulose-80C and Cellulose-140C) is enhanced compared to that of the Cellulose-RT. This is probably caused by cellulose intermolecular reorganization due to the new interchain hydrogen bonds formed after the desorption of water and glycerol.

3.3. Single gas permeation performances

Based on the same carbonization protocol described in Fig. 1, three types of cellulose hollow fiber precursors were carbonized at 600 °C to fabricate CMS membranes. The separation performances of the obtained CHFMs were firstly evaluated by a single gas permeation testing at 25 °C and 2 bar. It can be seen that gas permeabilities are mainly dependent on the gas kinetic diameter as shown in Fig. 4a, which indicates molecular sieving is the dominating transport mechanism for these carbon membranes. When the cellulose precursors were dried at a higher temperature, the derived carbon membranes (i.e., CHFM-80C and CHFM-140C) present a reduction of CO_2, O_2, N_2, and CH_4 permeabilities compared to the CHFM-RT prepared from the Cellulose-RT. However, it was found that the helium (He) permeability only slightly reduced from 450 to 403 barrer, which indicates that helium transport through these carbon membranes is not restricted by the reduced pore size. Since helium has negligible sorption on CMS micropores, the permeability is dominated by the helium diffusion coefficient, and the little variations on helium permeability probably indicate that all the three carbon membranes have similar open-pore channels (larger than 2.6 Å) for helium transportation. It is suspected that the drying treatment will shrink the pore size of cellulose precursors, but no additional pore collapse occurs when drying at higher temperatures, which confirms the importance of the applied glycerol-assisted drying process. Fig. 4b shows the enhanced selectivity of helium over the other gases for the CHFM-140C, which may indicate that the micropores of the prepared CHFMs are narrowed when increasing the drying temperature for cellulose hollow fiber precursors (see discussion in Section 3.4). Therefore, this carbon membrane may also have a potential for separation of light gases from heavy hydrocarbons such as helium recovery from natural gas.

3.4. Gas sorption and transport properties

To further investigate the micropore structures of prepared carbon membranes, pure CO_2 and CH_4 sorption at 25 °C of CHFMs were conducted, and the results are shown in Fig. 5. The DR equation fittings of CO_2 isotherm sorption as a function of pressure are given in Fig. 5a, which are used to calculate the structural parameters such as micropore volume (W_0), average pore size (L_0) and adsorption activation energy (E_0), as listed in Table 3. Following the increase of treatment temperature for the cellulose hollow fibers, the average pore size and micropore volume are reduced from 6 to 4.9 Å, and from 0.22 to 0.17 $cm^3\ g^{-1}$, respectively. The adsorption activation energy for CO_2, however, is increased from 29.4 to 33.2 kJ mol^{-1}. This indicates that the adsorbate-adsorbent interaction potential between carbon walls and CO_2 becomes weaker at a carbon structure with smaller pore size and micropore volume, which could be attributed to the fact that the pores are filled with CO_2 mainly by the mechanism of partial filling, instead of multilayer adsorption. The trends indicate that the microstructure of CHFMs can be tuned by modifying the structure and properties of cellulose hollow fiber precursors. Especially, the CHFM-140C presents a smaller average pore width compared to the CHFM-RT and the CHFM-80C as well as some other carbon membranes reported in the literature (see Table 3). As a result, the membrane selectivity was enhanced (see

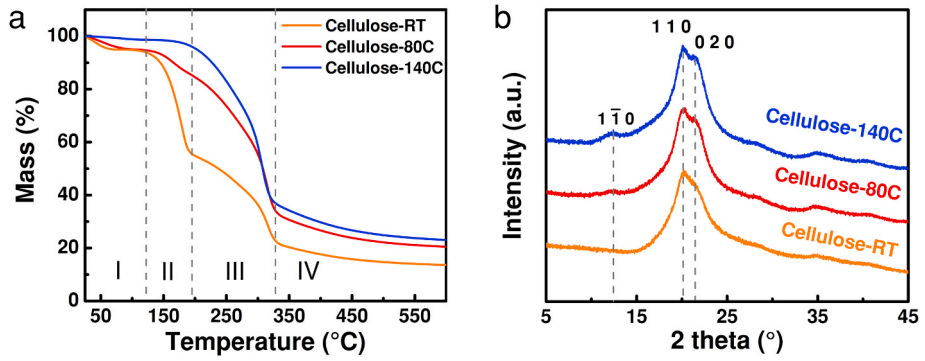

Fig. 3. a) TGA (I: release free water; II: release of bound water and glycerol; III cellulose degradation; IV: formation of carbon "plates"), and b) XRD of cellulose hollow fiber precursors.

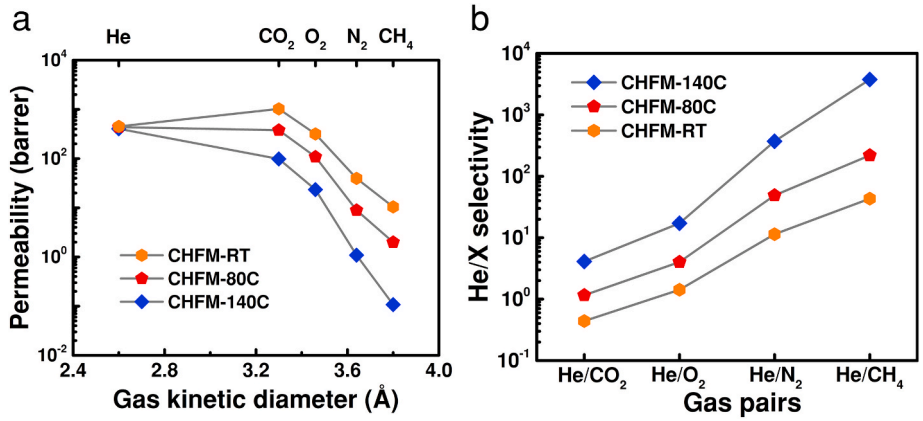

Fig. 4. Single gas permeation performance, a) gas permeabilities of CHFMs as a function of gas kinetic diameter at 25 °C and 2 bar, b) selectivity of He towards other gases.

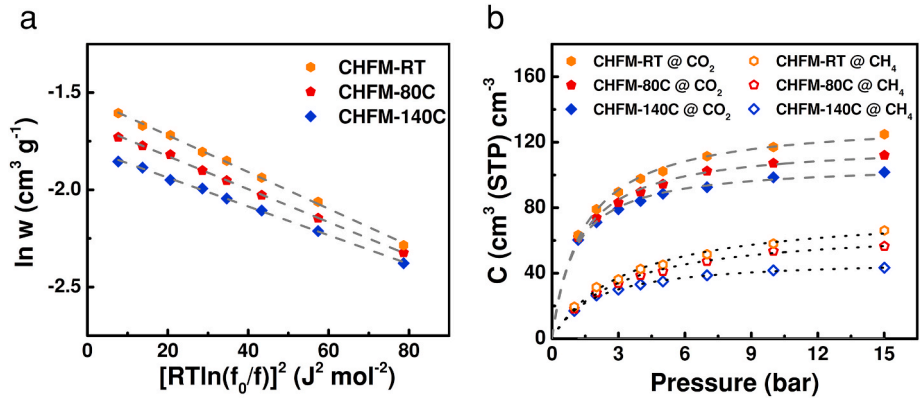

Fig. 5. a) DR fitting model based on CO_2 adsorption at 25 °C for the prepared CHFMs; b) pure gas CO_2 and CH_4 sorption isotherms at 25 °C of CHFMs, dash and dots lines are Langmuir fitting models for CO_2 and CH_4, respectively.

Table 3
Structural parameters of CHFMs calculated based on the DR equation and Stoeckli equation.

Parameters	CHFM-RT	CHFM-80C	CHFM-140C	CMSM1 [48]	CHFM [4]
E_0 (kJ mol^{-1})	29.4	31.0	33.2	31.6	31.4
L_0 (Å)	6.0	5.5	4.9	5.5	5.9
W_0 (cm^3 g^{-1})	0.22	0.19	0.17	0.28	0.15
True density (g cm^{-3})	1.35	1.42	1.54	1.6	-
Bulk density (g cm^{-3})	1.04	1.12	1.22	1.1	1.1

Table 4
Pure gas Langmuir isotherms parameters at 25 °C of CHFMs.

Langmuir isotherms parameters	CHFM-RT		CHFM-80C		CHFM-140C	
	CO_2	CH_4	CO_2	CH_4	CO_2	CH_4
$C_H^{'}$ (cm^3 (STP) cm^{-3})	139.9	78.4	119.4	67.7	106.8	48.7
b (bar^{-1})	0.71	0.30	0.82	0.34	1.00	0.54

Fig. 4). On the other hand, the reduction of CO_2 permeability can be explained by the decreased micropore volume and the increased adsorption activation energy.

Fig. 5b shows the Langmuir adsorption isotherms of CO_2 and CH_4 at 25 °C tested from 1 to 15 bar, and the model fitting parameters are listed in Table 4. The sorption capacities for both CO_2 and CH_4 decrease with the increase of the drying temperature for precursors. The gradually reduced Langmuir hole filling capacity $C_H^{'}$ (from 139.9 to 106.8 of cm^3 (STP) cm^{-3} for CO_2, and from 78.4 to 48.7 cm^3 (STP) cm^{-3} for CH_4) implies a reduced Langmuir sorption sites and tightened micropore structures [47], which is consistent with results obtained from the DR model.

The sorption coefficients of CO_2 and CH_4 at given pressures are determined by the secant slope of the sorption isotherm [47] as shown in Fig. 6a, where the applied sorption pressure is 2 bar (150 cmHg), the same value as the feed pressure of the single gas permeation measurements. The diffusion coefficients of CO_2 and CH_4, shown in Fig. 6b, are calculated by, $D_i = P_i/S_i$, in which P_i is the single gas permeability of component i at 2 bar. It can be found that the drying temperature for cellulose hollow fiber precursors has relatively little effect on the sorption coefficients of CO_2 and CH_4 of the derived carbon membranes, and only shows a slight reduction at higher drying temperature (see Fig. 5a). However, both the diffusion coefficients of CO_2 and CH_4 decrease with the increase of drying temperature. For instance, the diffusion coefficient of CO_2 decreased from 1.94×10^{-7} to 2.07×10^{-8} cm^2 s^{-1} when drying temperature increases from RT to 140 °C. Since the gas diffusion coefficient of CMS membranes reflects the packing of a carbon matrix [16,47], the reduced diffusion coefficients indicate that the carbon matrix is packed denser. This is consistent with the decrease of average pore size as indicated in Table 3. Moreover, the steep drop of CH_4 diffusion coefficient from 5.13×10^{-9} to 6.94×10^{-11} cm^2 s^{-1} implies that CH_4 molecules are excluded more strongly by the tightened micropores. Meanwhile, the CH_4 sorption was inhibited as the tightened micropores restrict CH_4 accessing the sorption sites of the carbon matrix.

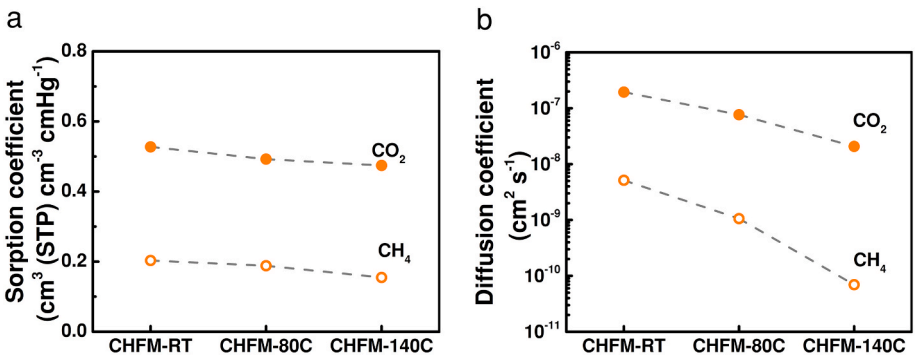

Fig. 6. a) Sorption coefficient and b) diffusion coefficient of CO_2 and CH_4 of CHFMs at 25 °Cand 2 bar.

Fig. 7 shows the diffusion and sorption selectivity enhancement for the carbon membranes made from high-temperature dried precursors compared to the reference of CHFM-RT. As the drying temperature increases from RT to 140 °C, the CO_2/CH_4 diffusion selectivity is enhanced by 7.9 times from 37.8 to 298.7, whereas the CO_2/CH_4 sorption selectivity also increases but has only 20% enhancement from 2.6 to 3.1. The overall contribution leads to the increase of CO_2/CH_4 permselectivity (the product of diffusion and sorption selectivity) from 98.1 to 917. It is worth noting that the diffusion selectivity is dominating the overall permselectivity of the CHFM-140C and presents the two orders of magnitude compared to the sorption selectivity. Therefore, gas translation diffusion through carbon molecular sieve membranes has a major contribution to gas permeation, whereas gas sorption has much less influence at a low operating pressure. However, one should expect that sorption contribution will increase at high pressure due to a quick reduction in CO_2 sorption compared to CH_4 sorption as indicated in Fig. 5b. The significantly improved CO_2/CH_4 permselectivity for CHFM-140C is mainly due to the narrower average pore size, down to 4.9 Å, which is also smaller than the carbon membranes reported in the literature [4,48].

3.5. Mixed gas separation performances

When natural gas sweetening is processed by a membrane system, it is necessary to avoid any water and HHCs condensation as those impurities may damage the membrane and reduce membrane performance significantly. Process simulation conducted by Baker and Lokhandwala [49] demonstrated that the single-phase of feed gas can be transformed into a two-phase region in the retentate due to the combination of Joule-Thomson effect (caused by CO_2 expansion permeating through membrane) and the increased HHCs levels. Elevating operating temperature or removing the impurities of water and HHCs would be a good solution to protect the membrane system. However, for most membrane materials, a higher operating temperature usually causes a reduction of gas separation factor, which reduces membrane separation efficiency. Thus, the capability of keeping attractive separation factors at relatively higher operating temperatures is essential. In this work, the mixed gas permeation measurements of CHFM-140C and CHFM-80C were carried out by 10 mol.% CO_2-90 mol.% CH_4 mixed gas at 60 °C and feed pressure from 10 to 50 bar, which was used to evaluate the potential for natural gas sweetening. It should be noted that testing at higher pressure of >50 bar has not been conducted in the current work due to the limitation on module sealing.

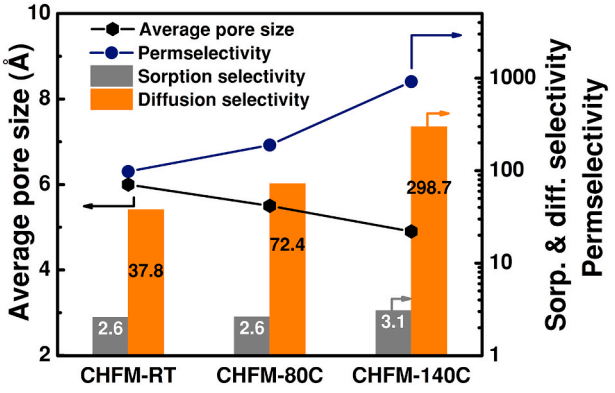

Fig. 7. CO_2/CH_4 sorption and diffusion selectivity of different CHFMs at 25 °C and 2 bar, permselectivity is the product of diffusion and sorption selectivity.

Fig. 8 summarizes the measured gas permeabilities and separation factors of CHFM-140C and CHFM-80C membranes. It was found that the CO_2 permeability slightly decreases from 177 to 126 barrer when the total feed pressure increases from 10 to 50 bar, while the CH_4 permeability shows relatively stable within the tested pressure range as shown in Fig. 8a. Regardless of this, the carbon membrane of CHFM-140C presents a remarkable CO_2/CH_4 separation factor of 131 at 60 °C and 50 bar from the mixed gas permeation measurement. To the best of our knowledge, this is the highest CO_2/CH_4 selectivity reported for self-supported carbon membranes under the high-pressure testing condition of 50 bar, which shows attractive potential for natural gas sweetening. On the other hand, though CHFM-80C has lower separation factor compared to that of CHFM-140C (see Fig. 8b), the ~3X higher CO_2 permeability of 333–550 barrer could be also promising to be used for the second-stage membrane unit where very high CO_2/CH_4 selectivity is not necessary due to a higher CO_2 content in feed gas (see Fig. S3). Process simulation based on the previous method [1,50] can be conducted to identify the optimal process configuration and operating condition-this is however not included in the current work.

It should be noted that the deviation of obtained separation factor as compared to the single gas permeation results is mainly due to the combination of higher testing temperature and pressure, as well as the well-known competitive component transport in mixed gas. Swaidan et al. [13] investigated the separation performances of CMS membranes by single gas and mixed gas (50 mol%CO_2-50 mol%CH_4) permeation at different pressures. They reported that pressure-dependent reduction in CH_4 permeability existed in single gas testing, while an opposite trend happened in the mixed gas permeation. As a result, up to 50% loss in CO_2/CH_4 separation factor for mixed gas testing was found compared to the ideal selectivity obtained from single gas permeation at the same partial pressure of 15 bar [13]. The reduction in CO_2 permeability with the increase of feed pressure can be explained by a competitive sorption effect [12,13]. When feed pressure increases gradually, the competitive sorption may become more significant as CH_4 has a much higher concentration and thus restricting the sorption sites for CO_2 [12], which leads to a reduction of CO_2 sorption coefficient at higher pressure (see Fig. S4). On the other hand, a small CO_2-induced dilation phenomenon of CMS materials may occur when increasing feed pressure [3]. The micropores and ultramicropores of CHFMs are expanded when they are

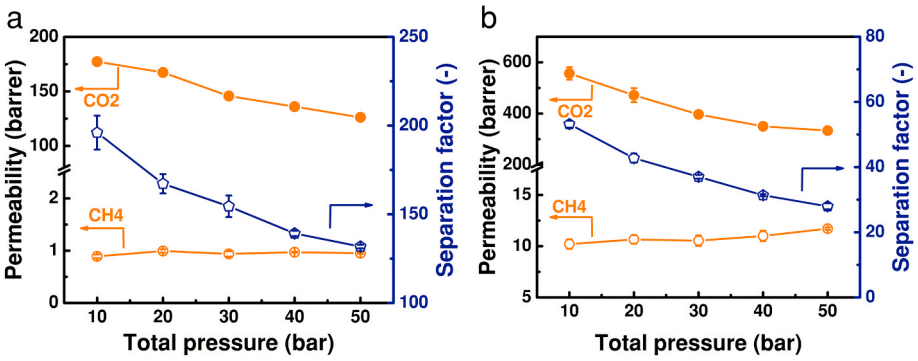

Fig. 8. Separation performances of a) CHFM-140C and b) CHFM-80C tested with a 10 mol.% CO_2-90 mol%CH_4 mixed gas under different feed pressures at 60 °C.

dilated resulting in the increase of diffusion coefficient of CO_2 and probably also CH_4. In addition, we further hypothesize that the dilation effect may have a more significant impact on bigger micropores since smaller micropores may provide significant resistance to counter the structure dilation. As shown in Fig. 8a (which is corresponding to smaller average micropores of 4.9 Å), the CH_4 permeability is mostly unchanged when the total pressure increases from 10 to 50 bar. Thus, the reduced CO_2/CH_4 separation factor is mainly caused by the reduction of CO_2 permeability. However, the CH_4 permeability of CHFM-80C (Fig. 8b, corresponding to larger average micropores of 5.5 Å) shows an increase of 14.8% when pressure increases from 10 to 50 bar. As a result, the CO_2/CH_4 separation factor dropped by 47% from 53 to 28. Recently, Zhang et al. [3] reported that CO_2/CH_4 separation factor of a CMS membrane slightly increased when testing pressure is over 800 psia (55 bar). They suggested that the densely packed CO_2 molecules in micropores (when pressure is above "threshold pressure" of 700–900 psia (42–62 bar)) might start to suppress CH_4 diffusion and thus offsetting the dilation effect [3]. For future work, mixed gas permeation measurement at higher pressures (e.g. 80–100 bar) can be conducted to investigate the dilation-induced influence on separation performance.

After mixed gas tests, the modules were exposed to the lab environment for ca. 6 months, and then tested by pure gases to investigate the aging phenomenon that normally exists in CMS membranes, which is caused by the physisorption or chemisorption between carbon matrix and oxygen or water molecules. As summarized in Table 5, the CO_2/CH_4 selectivity of CHFM-140C increased by 26.9% and CO_2 permeability dropped by 30.3% compared to the freshly prepared CHFM-140C. Similarly, the CO_2 permeability of CHFM-80C reduced by 23% while the CO_2/CH_4 selectivity increased slightly from 189 to 201. The difference of the selectivity loss between CHFM-80C and CHFM-140C can be explained by the narrower pores of CHFM-140C than that of the CHFM-80C. After being exposed to the air atmosphere, the adsorption of O_2 and water vapor in the micropores of membranes leads to a greater resistance for the permeated gases compared with the freshly prepared CHFMs. As a result, the gas permeabilities reduced about 23% and 30% for CHFM-80C and CHFM-140C, respectively. For the smaller micropores of CHFM-140C, the resistance effect to CH_4 molecules are even more significant compared to the CHFM-80C, which results in a considerable enhanced CO_2/CH_4 selectivity. It should be noted that the aging-caused 20–30% loss of CO_2 permeability is still competitive compared to the deacetylated cellulose acetate-derived CMS membranes [51].

4. Conclusion

In this work, highly CO_2 selective CMS membranes derived from cellulose hollow fiber precursors were successfully fabricated. By using a facile drying process for cellulose hollow fiber precursors, the resulted CMS membranes present enhanced separation performances. The denser structure of cellulose precursors obtained from a higher temperature drying process resulted in narrower micropores of CHFMs with reduced average pore width from 6 to 4.9 Å. This pretreatment led the carbon membrane of CHFM-140C to the enhancement of CO_2/CH_4 ideal selectivity up to 917 when tested at 2 bar. The separation performance of highly CO_2 selective CHFM-140C was further tested at high-pressure mixed gas of 10 mol%CO_2/90 mol%CH_4 at 60 °C, and a remarkable separation factor of 131 obtained at 50 bar shows attractive potential for natural gas sweetening. The gas permeability reduction of <30% after 6 months of exposure to the lab environment indicates good stability for the developed carbon membranes.

Table 5
The CO_2/CH_4 separation performances of CHFMs tested with pure gas at 2 bar and 25 °C before and after aging of ca. 6 months.

CMS membranes	CO_2 permeability (barrer)	CO_2/CH_4 selectivity
Fresh CHFM-80C	377	189
CHFM-80C, after aging	290	201
Fresh CHFM-140C	89	916
CHFM-140C, after aging	62	1162

CRediT authorship contribution statement

Linfeng Lei: Methodology, Investigation, Writing - original draft. **Arne Lindbråthen:** Methodology, Supervision, Writing - review & editing. **Xiangping Zhang:** Writing - review & editing. **Evangelos P. Favvas:** Writing - review & editing. **Marius Sandru:** Writing - review & editing. **Magne Hillestad:** Supervision, Writing - review & editing. **Xuezhong He:** Supervision, Project administration, Writing - review & editing.

Declaration of competing interest

The authors declare that they have no known competing financial interests or personal relationships that could have appeared to influence the work reported in this paper.

Acknowledgement

The authors acknowledge the Research Council of Norway (Norges forskningsråd) for funding this work in the CO2Hing project (#267615) through the Petromaks2 programme.

Appendix A. Supplementary data

Supplementary data to this article can be found online at https://doi.org/10.1016/j.memsci.2020.118529.

References

[1] X. He, I. Kumakiri, M. Hillestad, Conceptual Process Design and Simulation of Membrane Systems for Integrated Natural Gas Dehydration and Sweetening, Sep Purif Technol, 2020, 116993.

[2] R.W. Baker, Future directions of membrane gas separation technology, Ind. Eng. Chem. Res. 41 (2002) 1393–1411.

[3] M. Rungta, G.B. Wenz, C. Zhang, L. Xu, W. Qiu, J.S. Adams, W.J. Koros, Carbon molecular sieve structure development and membrane performance relationships, Carbon 115 (2017) 237–248.

[4] L. Lei, A. Lindbråthen, M. Hillestad, M. Sandru, E.P. Favvas, X. He, Screening cellulose spinning parameters for fabrication of novel carbon hollow fiber membranes for gas separation, Ind. Eng. Chem. Res. 58 (2019) 13330–13339.

[5] S. Yi, B. Ghanem, Y. Liu, I. Pinnau, W.J. Koros, Ultraselective glassy polymer membranes with unprecedented performance for energy-efficient sour gas separation, Sci. Adv. 5 (2019), eaaw5459.

[6] Y. Liu, Z. Liu, G. Liu, W. Qiu, N. Bhuwania, D. Chinn, W.J. Koros, Surprising plasticization benefits in natural gas upgrading using polyimide membranes, J. Membr. Sci. 593 (2020), 117430.

[7] G. Liu, V. Chernikova, Y. Liu, K. Zhang, Y. Belmabkhout, O. Shekhah, C. Zhang, S. Yi, M. Eddaoudi, W.J. Koros, Mixed matrix formulations with MOF molecular sieving for key energy-intensive separations, Nat. Mater. 17 (2018) 283–289.

[8] T. Rodenas, I. Luz, G. Prieto, B. Seoane, H. Miro, A. Corma, F. Kapteijn, F.X. Llabrés i Xamena, J. Gascon, Metal–organic framework nanosheets in polymer composite materials for gas separation, Nat. Mater. 14 (2015) 48–55.

[9] M.Z. Ahmad, T.A. Peters, N.M. Konnertz, T. Visser, C. Téllez, J. Coronas, V. Fila, W. M. de Vos, N.E. Benes, High-pressure CO_2/CH_4 separation of Zr-MOFs based mixed matrix membranes, Separ. Purif. Technol. 230 (2020), 115858.

[10] X. He, T.-J. Kim, M.-B. Hägg, Hybrid fixed-site-carrier membranes for CO_2 removal from high pressure natural gas: membrane optimization and process condition investigation, J. Membr. Sci. 470 (2014) 266–274.

[11] L. Deng, T.-J. Kim, M.-B. Hägg, Facilitated transport of CO_2 in novel PVAm/PVA blend membrane, J. Membr. Sci. 340 (2009) 154–163.

[12] D.Q. Vu, W.J. Koros, S.J. Miller, High pressure CO_2/CH_4 separation using carbon molecular sieve hollow fiber membranes, Ind. Eng. Chem. Res. 41 (2002) 367–380.

[13] R. Swaidan, X. Ma, E. Litwiller, I. Pinnau, High pressure pure- and mixed-gas separation of CO_2/CH_4 by thermally-rearranged and carbon molecular sieve membranes derived from a polyimide of intrinsic microporosity, J. Membr. Sci. 447 (2013) 387–394.

[14] L.M. Robeson, The upper bound revisited, J. Membr. Sci. 320 (2008) 390–400.

[15] X. He, M.-B. Hägg, T.-J. Kim, Hybrid FSC membrane for CO_2 removal from natural gas: experimental, process simulation, and economic feasibility analysis, AIChE J. 60 (2014) 4174–4184.

[16] C. Zhang, W.J. Koros, Ultraselective carbon molecular sieve membranes with tailored synergistic sorption selective properties, Adv. Mater. 29 (2017), 1701631.

[17] K. Hazazi, X. Ma, Y. Wang, W. Ogieglo, A. Alhazmi, Y. Han, I. Pinnau, Ultra-selective carbon molecular sieve membranes for natural gas separations based on a carbon-rich intrinsically microporous polyimide precursor, J. Membr. Sci. 585 (2019) 1–9.

[18] W. Qiu, J. Vaughn, G. Liu, L. Xu, M. Brayden, M. Martinez, T. Fitzgibbons, G. Wenz, W.J. Koros, Hyperaging tuning of a carbon molecular-sieve hollow fiber membrane with extraordinary gas-separation performance and stability, Angew. Chem. Int. Ed. 58 (2019) 11700–11703.

[19] J.S. Adams, A.K. Itta, C. Zhang, G.B. Wenz, O. Sanyal, W.J. Koros, New insights into structural evolution in carbon molecular sieve membranes during pyrolysis, Carbon 141 (2019) 238–246.

[20] O. Salinas, X. Ma, Y. Wang, Y. Han, I. Pinnau, Carbon molecular sieve membrane from a microporous spirobisindane-based polyimide precursor with enhanced ethylene/ethane mixed-gas selectivity, RSC Adv. 7 (2017) 3265–3272.

[21] J.A. Lie, M.-B. Hagg, Carbon membranes from cellulose: synthesis, performance and regeneration, J. Membr. Sci. 284 (2006) 79–86.

[22] X. He, M.-B. Hagg, Optimization of carbonization process for preparation of high performance hollow fiber carbon membranes, Ind. Eng. Chem. Res. 50 (2011) 8065–8072.

[23] M. Yoshimune, K. Haraya, Flexible carbon hollow fiber membranes derived from sulfonated poly(phenylene oxide), Separ. Purif. Technol. 75 (2010) 193–197.

[24] N.D. Alexopoulos, F.D. Gegitsidis, S.K. Kourkoulis, E.P. Favvas, Mechanical behavior of MWCNTs based mixed-matrix polymeric and carbon hollow fiber membranes, Separ. Purif. Technol. 183 (2017) 21–31.

[25] M. Kiyono, P.J. Williams, W.J. Koros, Effect of polymer precursors on carbon molecular sieve structure and separation performance properties, Carbon 48 (2010) 4432–4441.

[26] H.B. Park, Y.K. Kim, J.M. Lee, S.Y. Lee, Y.M. Lee, Relationship between chemical structure of aromatic polyimides and gas permeation properties of their carbon molecular sieve membranes, J. Membr. Sci. 229 (2004) 117–127.

[27] Y.-J. Fu, C.-C. Hu, D.-W. Lin, H.-A. Tsai, S.-H. Huang, W.-S. Hung, K.-R. Lee, J.-Y. Lai, Adjustable microstructure carbon molecular sieve membranes derived from thermally stable polyetherimide/polyimide blends for gas separation, Carbon 113 (2017) 10–17.

[28] E.P. Favvas, N.S. Heliopoulos, S.K. Papageorgiou, A.C. Mitropoulos, G. C. Kapantaidakis, N.K. Kanellopoulos, Helium and hydrogen selective carbon hollow fiber membranes: the effect of pyrolysis isothermal time, Separ. Purif. Technol. 142 (2015) 176–181.

[29] S.C. Rodrigues, M. Andrade, J. Moffat, F.D. Magalhães, A. Mendes, Preparation of carbon molecular sieve membranes from an optimized ionic liquid-regenerated cellulose precursor, J. Membr. Sci. 572 (2019) 390–400.

[30] T. He, I. Blume, A Process for Drying a Wet Porous Membrane Structure and the Porous Membrane Structure Obtained from Said Process, Patent, WO2004089520A1, in, 2003.

[31] J. Ji, M.J. Mehta, C. Dicecca, Hydrophilic Hollow Fiber Ultrafiltration Membranes that Include a Hydrophobic Polymer and a Method of Making These Membranes, Patent, WO02/076593A1, in, 2002.

[32] P.S. Barber, C.S. Griggs, G. Gurau, Z. Liu, S. Li, Z. Li, X. Lu, S. Zhang, R.D. Rogers, Coagulation of chitin and cellulose from 1-Ethyl-3-methylimidazolium acetate ionic-liquid solutions using carbon dioxide, Angew. Chem. Int. Ed. 52 (2013) 12350–12353.

[33] Y. Tomimatsu, H. Suetsugu, Y. Yoshimura, A. Shimizu, The solubility of cellulose in binary mixtures of ionic liquids and dimethyl sulfoxide: influence of the anion, J. Mol. Liq. 279 (2019) 120–126.

[34] D.L. Minnick, R.A. Flores, M.R. DeStefano, A.M. Scurto, Cellulose solubility in ionic liquid mixtures: temperature, cosolvent, and antisolvent effects, J. Phys. Chem. B 120 (2016) 7906–7919.

[35] E.O.A. Seoud, M. Kostag, K. Jedvert, N.I. Malek, Cellulose in ionic liquids and alkaline solutions: advances in the mechanisms of biopolymer dissolution and regeneration, Polymers 11 (2019) 1917.

[36] E.P. Favvas, G.C. Kapantaidakis, J.W. Nolan, A.C. Mitropoulos, N.K. Kanellopoulos, Preparation, characterization and gas permeation properties of carbon hollow fiber membranes based on Matrimid® 5218 precursor, J. Mater. Process. Technol. 186 (2007) 102–110.

[37] L. Segal, J.J. Creely, A.E. Martin, C.M. Conrad, An empirical method for estimating the degree of crystallinity of native cellulose using the X-ray diffractometer, Textil. Res. J. 29 (1959) 786–794.

[38] Y. Liu, Y. Nie, F. Pan, L. Zhou, X. Ji, Z. Kang, S. Zhang, Study on ionic liquid/cellulose/coagulator phase diagram and its application in green spinning process, J. Mol. Liq. 289 (2019), 111127.

[39] M.M. Dubinin, Generalization of the theory of volume filling of micropores to nonhomogeneous microporous structures, Carbon 23 (1985) 373–380.

[40] F. Stoeckli, A. Slasli, D. Hugi-Cleary, A. Guillot, The characterization of microporosity in carbons with molecular sieve effects, Microporous Mesoporous Mater. 51 (2002) 197–202.

[41] X. He, M.-B. Hägg, Structural, kinetic and performance characterization of hollow fiber carbon membranes, J. Membr. Sci. 390–391 (2012) 23–31.

[42] X. He, A. Lindbråthen, T.-J. Kim, M.-B. Hägg, Pilot testing on fixed-site-carrier membranes for CO_2 capture from flue gas, IJGGC 64 (2017) 323–332.

[43] G. Falca, V.-E. Musteata, A.R. Behzad, S. Chisca, S.P. Nunes, Cellulose hollow fibers for organic resistant nanofiltration, J. Membr. Sci. 586 (2019) 151–161.

[44] M. Chen, B. Coasne, R. Guyer, D. Derome, J. Carmeliet, Role of hydrogen bonding in hysteresis observed in sorption-induced swelling of soft nanoporous polymers, Nat. Commun. 9 (2018) 3507.

[45] I.P. Samayam, B.L. Hanson, P. Langan, C.A. Schall, Ionic-liquid induced changes in cellulose structure associated with enhanced biomass hydrolysis, Biomacromolecules 12 (2011) 3091–3098.

[46] J. Gong, J. Li, J. Xu, Z. Xiang, L. Mo, Research on cellulose nanocrystals produced from cellulose sources with various polymorphs, RSC Adv. 7 (2017) 33486–33493.

[47] S. Fu, G.B. Wenz, E.S. Sanders, S.S. Kulkarni, W. Qiu, C. Ma, W.J. Koros, Effects of pyrolysis conditions on gas separation properties of 6FDA/DETDA:DABA(3:2) derived carbon molecular sieve membranes, J. Membr. Sci. 520 (2016) 699–711.

[48] S. Lagorsse, F.D. Magalhães, A. Mendes, Carbon molecular sieve membranes: sorption, kinetic and structural characterization, J. Membr. Sci. 241 (2004) 275–287.

[49] R.W. Baker, K. Lokhandwala, Natural gas processing with Membranes: an overview, Ind. Eng. Chem. Res. 47 (2008) 2109–2121.

[50] Y. Chu, X. He, Process simulation and cost evaluation of carbon membranes for CO_2 removal from high-pressure natural gas, Membranes 8 (2018) 118.

[51] S. Haider, A. Lindbråthen, J.A. Lie, M.-B. Hägg, Regenerated cellulose based carbon membranes for CO_2 separation: durability and aging under miscellaneous environments, J. Ind. Eng. Chem. 70 (2019) 363–371.